Selection rules for single-chain-magnet behaviour in non-collinear Ising systems

2009 J. Phys.: Condens. Matter 21 236007

(http://iopscience.iop.org/0953-8984/21/23/236007)

IOP Publishing Journal of Physics: Condensed Matter

J. Phys.: Condens. Matter **21** (2009) 236007 (15pp) doi:10.1088/0953-8984/21/23/236007

Selection rules for single-chain-magnet behaviour in non-collinear Ising systems

Alessandro Vindigni[1] **and Maria Gloria Pini**[2]

[1] Laboratorium für Festkörperphysik, ETH Zürich, CH-8093 Zürich, Switzerland
[2] Istituto dei Sistemi Complessi, Consiglio Nazionale delle Ricerche, Via Madonna del Piano 10, I-50019 Sesto Fiorentino (FI), Italy

E-mail: vindigni@phys.ethz.ch

Received 11 March 2009
Published 13 May 2009
Online at stacks.iop.org/JPhysCM/21/236007

Abstract

The magnetic behaviour of molecular single-chain magnets is investigated in the framework of a one-dimensional Ising model with single spin-flip Glauber dynamics. Opportune modifications to the original theory are required in order to account for non-collinearity of local anisotropy axes between themselves and with respect to the crystallographic (laboratory) frame. The extension of Glauber's theory to the case of a collinear Ising ferrimagnetic chain is also discussed. Within this formalism, both the dynamics of magnetization reversal in zero field and the response of the system to a weak magnetic field, oscillating in time, are studied. Depending on the experimental geometry, selection rules are found for the occurrence of slow relaxation of the magnetization at low temperatures, as well as for resonant behaviour of the a.c. susceptibility as a function of temperature at low frequencies. The present theory applies successfully to some real systems, namely Mn-, Dy- and Co-based molecular magnetic chains, showing that single-chain-magnet behaviour is not only a feature of collinear ferro- and ferrimagnetic, but also of canted antiferromagnetic chains.

(Some figures in this article are in colour only in the electronic version)

1. Introduction

Slow dynamics of magnetization reversal is a crucial requirement for potential applications of single-chain magnets (SCMs) [1–3], and nanowires in general, in magnetic-memory manufacture. In nanowires with a biaxial anisotropy this phenomenon is governed by thermal nucleation and propagation of non-uniform solutions of the corresponding Euler–Lagrange equation, provided that the sample length is much larger than the domain-wall width. The associated characteristic time is expected to follow an Arrhenius law [4, 5]. For genuine one-dimensional (1D) Ising systems with single spin-flip stochastic dynamics, a slow relaxation of the magnetization was first predicted by Glauber [6] in 1963. Through Glauber's approach, many physical systems were investigated, ranging from dielectrics [7–9] to polymers [7, 10, 11]. More fundamentally, this model has been employed to justify the use of the Kohlrausch–Williams–Watts function [10, 12] (stretched exponential) to fit the relaxation of generalized 1D spin systems. Also the universality issue of the dynamic critical exponent [13–17] of the Ising model [18], as well as strongly out-of-equilibrium processes (magnetization reversal, facilitated dynamics, etc [19]) have been studied moving from the basic ideas proposed by Glauber.

In this paper, single spin-flip Glauber dynamics is used to investigate theoretically the slow dynamics of magnetization reversal in molecular magnetic systems. In particular, we extend Glauber's theory [6] both to a collinear Ising ferrimagnetic chain, and to a chain in which non-collinearity of local anisotropy axes is encountered. Such extensions are motivated by the fact that (i) in molecular-based realizations of SCMs, antiferromagnetic coupling typically has a larger intensity than the ferromagnetic one; in fact, the overlapping of magnetic orbitals, which implies antiferromagnetic exchange interaction between neighbouring spins, can be more easily obtained than the orthogonality condition, leading to ferromagnetism [20–22]; and (ii) non-collinearity between local anisotropy axes and the crystallographic (laboratory) frame takes place quite often in molecular spin chains. Besides magnetization reversal, the dynamic response of the system to a weak magnetic field, oscillating in time at a frequency ω, is also studied. Depending on the specific experimental

geometry, selection rules are found for the occurrence of resonant behaviour of the a.c. susceptibility as a function of temperature (stochastic resonance) at low frequencies, as well as for slow relaxation of the magnetization in zero field at low temperatures.

It is worth noticing that, for zero applied field, the kinetic Ising model first proposed by Glauber and solved by him in one dimension [6] can be mapped, in any dimension D, onto an Ising model with multispin interactions in a *transverse* field [23]. For D = 1, the latter quantum spin Hamiltonian could be diagonalized after a Jordan–Wigner transformation [24], and the eigenvalues of the equivalent fermion problem were shown [23] to coincide with the inverse of the characteristic timescales of the original stochastic model [6]. Since then, a wealth of papers have appeared [25, 26], where the techniques of quantum field theory on a lattice have been used to examine stochastic processes of particles in a solid (and other *non*-quantum mechanical objects, like domain walls in a magnet). In this way, exact solutions of the master equation could be obtained, in 1D, in terms of the energy spectrum of the equivalent quantum Hamiltonian. In the present paper, we prefer to follow Glauber's theoretical approach (modified in order to include the effect of non-collinearity) because our aim is primarily to explain the selection rules for single-chain-magnet behaviour, experimentally observed in real molecular compounds. For such systems, the original solution [6] of the master equation in terms of classical spins is—in our opinion—more transparent than a quantum-field-theoretical approach, and thus it is expected to be more useful to the experimental community of molecular magnetism.

This paper is organized as follows. In section 2 we recall some basic results of the original Glauber theory [6] and introduce our model, which allows computing the a.c. susceptibility of a chain of coupled non-collinear anisotropic magnetic centres, possibly with Landé factors that vary from site to site. In section 3 we calculate, in a linear approximation, the magnetic response of the system to a weak, oscillating magnetic field. For a chain of N spins, the a.c. susceptibility is expressed as the superposition of N contributions, each characterized by its timescale; through a few simple examples, we show that, depending on the geometry of the system (i.e. the relative orientations of the local easy anisotropy axes and of the applied field), different timescales can be selected, possibly giving rise, for low frequencies, to a resonant peak in the temperature dependence of the complex magnetic susceptibility. In section 4 we show that the theory provides a satisfactory account for the SCM behaviour selectively observed in some magnetic molecular chain compounds, characterized by dominant antiferromagnetic exchange interactions and non-collinearity between spins. Finally, in section 5, the conclusions are drawn and possible forthcoming applications are also discussed. In the three appendices one can find details about the calculation of the a.c. susceptibility and the relaxation rate of the magnetization in zero field.

2. The non-collinear Ising–Glauber model

In a celebrated paper [6], Glauber introduced, in the usual 1D Ising model [18], a stochastic dependence on the time variable t: i.e. the state of a spin lying on the kth lattice site was represented by a two-valued stochastic function $\sigma_k(t)$:

$$\mathcal{H}_{\mathrm{I}} = -\sum_{k=1}^{N} (J_{\mathrm{I}}\sigma_k\sigma_{k+1} + g\mu_{\mathrm{B}}H\mathrm{e}^{-\mathrm{i}\omega t}\sigma_k), \qquad \sigma_k(t) = \pm 1. \tag{2.1}$$

J_{I} is the exchange coupling constant, that favours nearest-neighbouring spins to lie parallel ($J_{\mathrm{I}} > 0$, ferromagnetic exchange) or antiparallel ($J_{\mathrm{I}} < 0$, antiferromagnetic exchange), g is the Landé factor of each spin and μ_{B} is the Bohr magneton. In the original paper [6], a system of equivalent magnetic centres, arranged in a 1D lattice in such a way that the easy axis direction was the same for all of them (collinear Ising chain), was studied. Moreover, the response to a time-dependent magnetic field $H(t)$, applied parallel to the common easy axis direction and oscillating with frequency ω, as in typical a.c. susceptibility experiments, was considered [6].

In order to investigate the phenomena of slow relaxation (for $H = 0$) and resonant behaviour of the a.c. susceptibility (for $H \neq 0$) in molecular SCMs, we are going to generalize the Glauber model (2.1) accounting for the non-collinearity of local anisotropy axes between themselves and with respect to the crystallographic (laboratory) frame. To this aim, we adopt the following model Hamiltonian:

$$\mathcal{H} = -\sum_{k=1}^{N} (J_{\mathrm{I}}\sigma_k\sigma_{k+1} + G_k\mu_{\mathrm{B}}H\mathrm{e}^{-\mathrm{i}\omega t}\sigma_k), \qquad \sigma_k(t) = \pm 1. \tag{2.2}$$

J_{I} is an effective Ising exchange coupling that can approximately be related to the Hamiltonian parameters of a real SCM [27, 28]: see later on the discussion in section 4. Like in the usual Ising–Glauber collinear model (2.1), the spins in (2.2) are described by classical one-component vectors that are allowed to take two integer values $\sigma_k(t) = \pm 1$, but now the magnetic moments may be oriented along different directions, $\hat{\mathbf{z}}_k$, varying from site to site. Within this scheme, the Landé tensor of a spin on the kth lattice site has just a non-zero component, $g_k^{\parallel}$, along the local easy anisotropy direction $\hat{\mathbf{z}}_k$. Denoting by $\hat{\mathbf{e}}_H$ the direction of the oscillating magnetic field, $\mathbf{H}(t) = H\mathrm{e}^{-\mathrm{i}\omega t}\hat{\mathbf{e}}_H$, we define the generalized Landé factor G_k appearing in (2.2) as

$$G_k = g_k^{\parallel}\,\hat{\mathbf{z}}_k \cdot \hat{\mathbf{e}}_H \tag{2.3}$$

i.e. a scalar quantity that varies from site to site. Following Glauber [6], we define the single-spin expectation value $s_k(t) = \langle\sigma_k\rangle_t$, where brackets denote a proper ensemble average and the stochastic magnetization along the direction of the applied field

$$\langle M\rangle_t = \mu_{\mathrm{B}}\sum_{k=1}^{N} G_k\langle\sigma_k\rangle_t = \mu_{\mathrm{B}}\sum_{k=1}^{N} G_k s_k(t). \tag{2.4}$$

The basic equation of motion of the Glauber model [12, 14] is

$$\frac{\mathrm{d}}{\mathrm{d}t}s_k(t) = -2\langle\sigma_k w_{\sigma_k\to-\sigma_k}\rangle, \tag{2.5}$$

in which $w_{\sigma_k\to-\sigma_k}$ represents the probability per unit time to reverse the kth spin, through the flip $+\sigma_k \to -\sigma_k$. For a system of N coupled spins, this probability is affected by the interaction with the other spins, with the thermal bath and, possibly, with an external magnetic field. Among all possible choices for the transition probability $w_{\sigma_k\to-\sigma_k}$ as a function of the $N+1$ variables [11, 19, 29, 30] $\{\sigma_1,\ldots,\sigma_k,\ldots,\sigma_N,t\}$, we adopt, in zero field and in the presence of an external field, respectively:

$$w^{H=0}_{\sigma_k\to-\sigma_k} = \tfrac{1}{2}\alpha[1-\tfrac{1}{2}\gamma\sigma_k(\sigma_{k-1}+\sigma_{k+1})], \tag{2.6}$$

$$w^{H}_{\sigma_k\to-\sigma_k} = w^{H=0}_{\sigma_k\to-\sigma_k}(1-\delta_k\sigma_k). \tag{2.7}$$

The attempt frequency $\frac{1}{2}\alpha$ (i.e. the probability per unit time to reverse an isolated spin) remains an undetermined parameter of the model; γ accounts for the effect of the two nearest neighbours of the kth spin; the parameters δ_k have the role of stabilizing the configuration in which the kth spin is parallel to the field and destabilizing the antiparallel configuration. Thanks to the particular choices (2.6) and (2.7) for the transition probability, by imposing the detailed balance conditions [6] it is possible to express γ and δ_k as functions of the parameters in the spin Hamiltonian (2.2):

$$\gamma = \tanh(2\beta J_{\mathrm{I}}), \qquad \delta_k = \tanh(\beta G_k\mu_{\mathrm{B}}H), \tag{2.8}$$

where $\beta = \frac{1}{k_{\mathrm{B}}T}$ is the inverse temperature in units of Boltzmann's constant. For $H=0$, combining (2.5) with (2.6) yields

$$\frac{\mathrm{d}\underline{s}(t)}{\mathrm{d}t} = -\alpha\mathbf{A}\underline{s}(t), \tag{2.9}$$

where $\underline{s}(t)$ denotes the vector of single-spin expectation values $\{s_1(t),\ s_2(t),\ldots,\ s_N(t)\}$ and $\mathbf{A}$ is a square $N\times N$ symmetric matrix, whose non-zero elements are $A_{k,k}$ =1 and $A_{k,k-1} = A_{k,k+1} = -\frac{\gamma}{2}$, with $A_{1,N} = A_{N,1} = -\frac{\gamma}{2}$ if periodic boundary conditions are assumed for the N-spin chain. A closed solution of the set of first-order differential equations (2.9) can be obtained expressing the expectation value of each spin, $s_k(t)$, in terms of its spatial Fourier transform (FT) $\tilde{s}_q$:

$$s_k(t) = \sum_q \tilde{s}_q \mathrm{e}^{\mathrm{i}qk}\mathrm{e}^{-\lambda_q t}. \tag{2.10}$$

By substituting (2.10) into (2.9), one readily obtains the dispersion relation

$$\lambda_q = \alpha(1-\gamma\cos q), \qquad q = \frac{2\pi}{N}n \tag{2.11}$$

with $n = 0,\ 1,\ldots,\ N-1$ [31]. For ferromagnetic coupling ($J_{\mathrm{I}}>0$, hence $\gamma>0$) the smallest eigenvalue $\lambda_{q=0} = \alpha(1-\gamma)$ occurs for $n=0$, independently of the number of spins N in the chain. For antiferromagnetic coupling ($J_{\mathrm{I}}<0$, hence $\gamma<0$) and N even, the smallest eigenvalue $\lambda_{q=\pi} = \alpha(1-|\gamma|)$ occurs for $n = \frac{N}{2}$; while in the case of N odd, the smallest eigenvalue corresponds to $\alpha[1-|\gamma|\cos(\frac{\pi}{N})]$, thus depending on the number of spins in the antiferromagnetic chain [32]. The characteristic timescales of the system, τ_q, are given by

$$\tau_q = \frac{1}{\lambda_q} = \frac{1}{\alpha(1-\gamma\cos q)}. \tag{2.12}$$

At finite temperatures, the characteristic times τ_q are finite because $|\gamma|<1$; for $T\to 0$ one has that $1-|\gamma|$ vanishes irrespective of the sign of J_{I}, because $\gamma\to\frac{J_{\mathrm{I}}}{|J_{\mathrm{I}}|} = \pm 1$. Thus, for $H=0$, there is always one diverging timescale in the $T\to 0$ limit: $\tau_{q=0}$ for ferromagnetic coupling and $\tau_{q=\pi}$ for antiferromagnetic coupling (and even N). In the presence of a non-zero, oscillating field $H(t) = H\mathrm{e}^{-\mathrm{i}\omega t}$, the equation of motion (2.5) with the choice (2.7) takes a form (see (3.1) in section 3 later on) which can still be solved, though in an approximate way [6], for a sufficiently weak intensity of the applied magnetic field.

3. Magnetic response to an oscillating magnetic field

In this section we discuss the magnetic response of a non-collinear Ising chain to a weak a.c. field. In spite of its intrinsic simplicity, our approach naturally justifies the occurrence of resonant behaviour only for fields applied along specific directions with respect to the crystallographic axes of a molecular compound, as observed in experiments [33–37].

In the presence of a magnetic field H, the transition probability to be put in the equation of motion (2.5) is $w^{H}_{\sigma_k\to-\sigma_k}$, defined in (2.7). One obtains

$$\frac{\mathrm{d}s_k(t)}{\mathrm{d}t} = -\alpha\Big\{s_k(t) - \frac{\gamma}{2}[s_{k+1}(t)+s_{k-1}(t)] + \frac{\gamma\delta_k}{2}[\langle\sigma_k\sigma_{k+1}\rangle_t + \langle\sigma_{k-1}\sigma_k\rangle_t] - \delta_k\Big\} \tag{3.1}$$

i.e. the presence of a non-zero field introduces into the equation of motion both a non-homogeneous term, δ_k, and the time-dependent pair-correlation functions $\langle\sigma_k\sigma_{k\pm1}\rangle_t$. The latter ones, assuming that the field is weak enough to induce just small departures from equilibrium, can be approximated by their time-independent counterparts [38]:

$$\langle\sigma_k\sigma_{k+1}\rangle_t = \langle\sigma_{k-1}\sigma_k\rangle_t \approx \tanh(\beta J_{\mathrm{I}}) \equiv \eta. \tag{3.2}$$

As is usual in a.c. susceptibility measurements, we also assume the time-dependent magnetic field $\mathbf{H}(t) = H\mathrm{e}^{-\mathrm{i}\omega t}\hat{\mathbf{e}}_H$, oscillating at a frequency ω, to be weak so that the δ_k parameters can be linearized. Within this linear approximation (see appendix A for details), the susceptibility of a non-collinear Ising chain is

$$\chi(\omega,T) = N\mu_{\mathrm{B}}^2\beta f(\beta J_{\mathrm{I}})\sum_q \frac{\alpha|\tilde{G}_q|^2}{\alpha(1-\gamma\cos q)-\mathrm{i}\omega}, \tag{3.3}$$

where $f(\beta J_{\mathrm{I}}) = 1-\gamma\eta = \frac{1-\eta^2}{1+\eta^2}$ and $\tilde{G}_q$ is the FT of G_k. In principle, the a.c. susceptibility of a chain with N spins admits N poles, corresponding to the N eigenvalues λ_q in (2.11). Each mode is related to a different timescale $\tau_q = 1/\lambda_q$. In practice, not all the timescales will be involved in the complex

susceptibility $\chi(\omega, T)$, but *only the ones selected* by $\tilde{G}_q$. A result similar, at first glance, to (3.3) was deduced by Suzuki and Kubo [31], but in their case the relationship was between the timescale τ_q and the wavevector-dependent susceptibility $\chi(q, \omega)$. In contrast, in an a.c. susceptibility experiment only the zero-wavevector susceptibility $\chi(q = 0, \omega)$ is accessible; the peculiarity of (3.3) is that other timescales, different from $\tau_{q=0}$, can be selected, due to the dependence of the gyromagnetic factors G_k and of the local anisotropy axes on the site position k. This is the main result of our study and will be clarified hereafter through a few examples of non-collinear geometries, selected according to the most frequent realizations in molecular magnetic polymers.

3.1. The a.c. susceptibility of a collinear Ising ferrimagnetic chain

Let us start considering the case of a one-dimensional Ising model with two kinds of spins (aligned parallel or antiparallel to the chain axis) alternating on the odd and even magnetic sites of the lattice with Landé factors $G_{2r+1} = g_o$ and $G_{2r} = g_e$ (integer r), respectively. Strictly speaking, a collinear Ising ferrimagnet is characterized by an antiferromagnetic coupling $J_I < 0$, but also the case $J_I > 0$ can be treated through (3.3). In fact, since the local axis of anisotropy has the same direction for all the spins, the FT of the site-dependent Landé factor is

$$\tilde{G}_q = \frac{1}{N}\sum_{r=1}^{N/2}[g_e e^{-iq2r} + g_o e^{-iq(2r-1)}] = (g_e + e^{iq} g_o)\frac{1}{N}\sum_{r=1}^{N/2} e^{-iq2r}. \tag{3.4}$$

Taking into account that, in the presence of periodic boundary conditions, one has

$$\sum_{r=1}^{N/2} e^{-iq2r} = \frac{N}{2}(\delta_{q,0} + \delta_{q,\pi}), \tag{3.5}$$

it follows that the only non-zero values of $\tilde{G}_q$ are for $q = 0$ and π:

$$\tilde{G}_q^{\parallel} = \tfrac{1}{2}[(g_e + g_o)\delta_{q,0} + (g_e - g_o)\delta_{q,\pi}]. \tag{3.6}$$

Thus, according to (3.3), the parallel a.c. susceptibility ($\parallel = zz$) of a collinear Ising chain with alternating spins is

$$\chi_{\parallel}(\omega, T) = N\mu_B^2 \beta f(\beta J_I) \times \frac{1}{4}\left[\frac{(g_e + g_o)^2}{(1-\gamma) - i(\frac{\omega}{\alpha})} + \frac{(g_e - g_o)^2}{(1+\gamma) - i(\frac{\omega}{\alpha})}\right]. \tag{3.7}$$

It appears that both the relaxation times obtained by Suzuki and Kubo [31] for the ordinary and the staggered susceptibility of the usual Ising model, namely $\tau_{q=0} = [\alpha(1-\gamma)]^{-1}$ and $\tau_{q=\pi} = [\alpha(1+\gamma)]^{-1}$, respectively, do coexist in the a.c. susceptibility (3.7). Notice that, in the $\omega \to 0$ limit, the static susceptibility of the Ising ferrimagnet in zero field [17] is recovered from (3.7), since one has $\frac{f(\beta J_I)}{1\mp\gamma} = \frac{1-\eta^2}{1+\eta^2}\frac{1}{1\mp\gamma} = e^{\pm 2\beta J_I}$.

As regards the dynamic response of the system to an oscillating magnetic field applied along the chain axis, depending on the sign of the effective exchange coupling constant J_I, either the ferromagnetic ($g_e + g_o$) or the antiferromagnetic ($g_e - g_o$) branch of the parallel susceptibility (3.7) is characterized by a diverging timescale at low temperature. In particular, for a collinear Ising ferrimagnet one has $J_I < 0$, so that $\tau_{q=\pi}$ is diverging, while $\tau_{q=0}$ is short (of the order of α^{-1}, the attempt frequency of an isolated spin). Thus, for $J_I < 0$, a resonant behaviour of the a.c. susceptibility versus temperature (at low frequencies $\omega/\alpha \ll 1$) can only be observed in the case $g_e \neq g_o$ (see figure 1(d)) when magnetic moments are *uncompensated*, while a broad peak is found in the case $g_e = g_o$ when the net magnetization is zero (see figure 1(b)). Clearly, for $J_I > 0$, a resonant peak is found in both cases (see figures 1(a) and (c)), because a net magnetization is always present in the system.

Such a resonant behaviour of the a.c. susceptibility versus T, in ferromagnetic [39] as well as in ferrimagnetic [17] Ising chains with single spin-flip Glauber dynamics, is a manifestation of the stochastic resonance phenomenon [40]: i.e. the response of a set of coupled bistable systems to a periodic excitation is enhanced in the presence of a stochastic noise when a matching occurs between the fluctuation-induced switching rate of the system and the forcing frequency. In a magnetic chain, the role of stochastic noise is played by thermal fluctuations and the resonant peak in the temperature dependence of the a.c. susceptibility occurs when the statistical timescale, associated with the slow decay of the magnetization, matches with the deterministic timescale of the applied magnetic field:

$$\tau_q(T_{peak}) \approx \frac{1}{\omega}. \tag{3.8}$$

For completeness, the reader can refer to appendix C and section 4.4 for details about the ferrimagnetic-chain relaxation in zero field starting from 'partial' and full saturation.

3.2. The a.c. susceptibility of a twofold helix

The helical arrangement of local axes of anisotropy, $\hat{\mathbf{z}}_k$, which thus realize reciprocal non-collinearity between them, is often encountered in real systems [1, 3]. Details for the general case and for the definition of the crystallographic axes (x, y, z) are given in appendix B. As a general result, the susceptibility for fields applied along the unique axis of the helix (i.e. the chain axis), z, is given by

$$\chi_{\parallel}(\omega, T) = N\mu_B^2 \beta f(\beta J_I)\frac{g^2 \cos^2\theta}{(1-\gamma) - i(\frac{\omega}{\alpha})} \tag{3.9}$$

which differs from Glauber's result for the collinear Ising chain [6] only by the geometrical factor $\cos^2\theta$. For ferromagnetic coupling, $J_I > 0$, the relaxation time $\tau_0 = [\alpha(1-\gamma)]^{-1}$ diverges as $T \to 0$, and a resonant behaviour of the a.c. parallel susceptibility versus temperature is found, at low frequency, when the oscillating field is applied parallel to the helix axis, z, along which spins are *uncompensated*: see figure 2(a), which refers to the case of a twofold helix ($n = 2$ with the notation of appendix B).

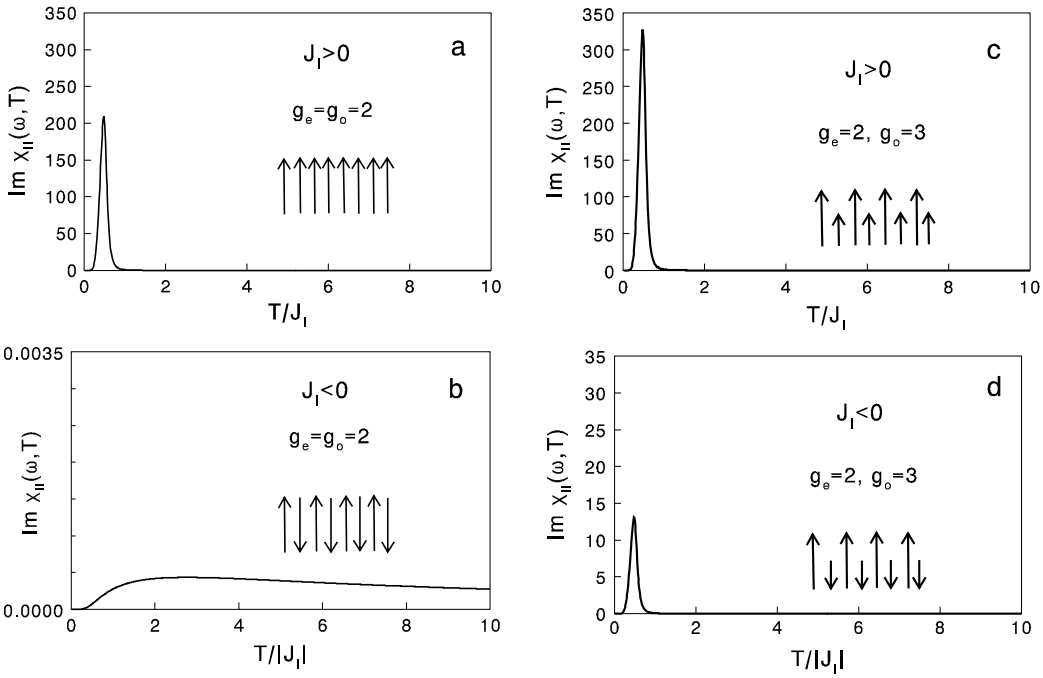

Figure 1. Temperature dependence of the imaginary part of the complex susceptibility, (3.7), of a collinear one-dimensional Ising model with alternating spins. Resonant behaviour in response to an oscillating magnetic field is possible, at low frequency, only when magnetic moments are uncompensated ((a), (c), (d)), while a broad peak is found when the net magnetization is zero (b). (The curves refer to reduced frequency $\omega/\alpha = 0.001$.)

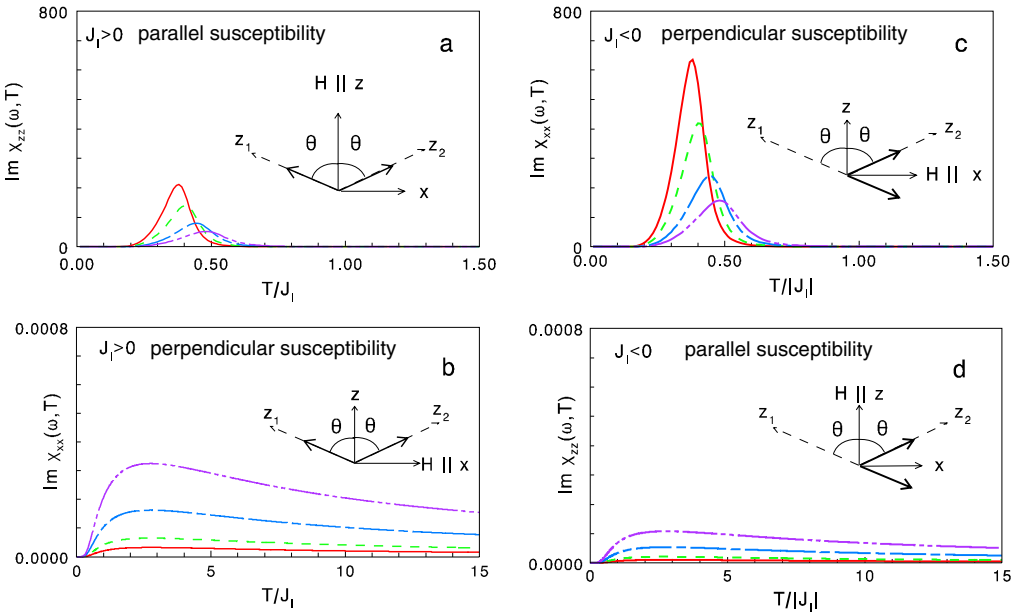

Figure 2. (Colour online) Temperature dependence of the imaginary part of the parallel (3.9) and perpendicular (3.11) complex susceptibility of an Ising chain with twofold helical spin arrangement. The local axes $\hat{\mathbf{z}}_1$ and $\hat{\mathbf{z}}_2$ were assumed to form an angle $\theta = \frac{\pi}{3}$ with z, the chain axis (unique axis of the helix). Different curves refer to different values of ω/α: 0.0001 (continuous, red line); 0.0002 (dashed, green line); 0.0005 (dashed single-dotted, blue line) and 0.0010 (dashed double-dotted, violet line). Resonant behaviour in response to an oscillating magnetic field is possible, at low frequency, only for a field applied in a direction where magnetic moments are uncompensated ((a), (c)), while a broad peak is found ((b), (d)) when there is no net magnetization along the field direction.

Let us now consider the case of an oscillating magnetic field H applied perpendicularly to the chain axis. Here we consider only the case $n = 2$, but the reader is referred to appendix B for $n > 2$.

- $n = 2$. In this case, it is worth noticing that, for H parallel to y, one has identically $G_r \equiv 0$ for any lattice site r. Thus, $\tilde{G}^y_q \equiv 0$ and the corresponding a.c. susceptibility is identically zero: $\chi_{yy}(\omega, T) \equiv 0$ (not shown). In contrast,

for H parallel to x, one has $G_r = -g\sin\theta$ on odd sites and $G_r = +g\sin\theta$ on even sites. The FT is

$$\tilde{G}^x_q = \frac{1}{N}\sum_{r=1}^{N/2} g\sin\theta(\mathrm{e}^{-\mathrm{i}q2r} - \mathrm{e}^{-\mathrm{i}q(2r-1)})$$
$$= g\sin\theta\frac{\delta_{q,0}+\delta_{q,\pi}}{2}(1-\mathrm{e}^{\mathrm{i}q}) = g\sin\theta\,\delta_{q,\pi} \qquad (3.10)$$

where we have taken into account (3.5). Thus, for ferromagnetic coupling, $J_\mathrm{I} > 0$, the relaxation time $\tau_\pi = [\alpha(1+\gamma)]^{-1}$ does not diverge as $T \to 0$ and the perpendicular a.c. susceptibility

$$\chi_{xx}(\omega, T) = N\mu_\mathrm{B}^2\beta f(\beta J_\mathrm{I})\frac{g^2\sin^2\theta}{(1+\gamma) - \mathrm{i}(\frac{\omega}{\alpha})} \qquad (3.11)$$

does not present a resonant behaviour as a function of temperature; rather, it presents a broad maximum (see figure 2(b)). Clearly, in the case of antiferromagnetic coupling, $J_\mathrm{I} < 0$, the behaviour of the susceptibility components is reversed: a broad maximum is found for the temperature dependence of the parallel susceptibility $\chi_{zz}(\omega, T)$ (see figure 2(d)), while a resonant behaviour is found for the perpendicular susceptibility $\chi_{xx}(\omega, T)$ (see figure 2(c)).

In appendix B, we show that no resonant behaviour is expected for the perpendicular a.c. susceptibility $\chi_\perp(\omega, T)$ of an n-fold helix with $n > 2$, neither for $J_\mathrm{I} > 0$ nor for $J_\mathrm{I} < 0$. Such a remarkable result is consistent with what was observed in the CoPhOMe molecular spin chain (see section 4.3), and it may be of interest for further experimental studies on the dynamics of other molecular magnets.

Summarizing, in the general case of an Ising chain with an n-fold helical spin arrangement ($n \geqslant 2$), we have explicitly shown that a resonant behaviour of the a.c. susceptibility versus temperature, similar to the one displayed by ferromagnetic [6, 39] and ferrimagnetic [17] Ising chains with collinear spins, is possible only for a field applied in a direction where magnetic moments are *uncompensated*. In contrast, a broad peak is found when there is no net magnetization along the field direction in the limit $T \to 0$ and $H \to 0^+$.

4. Application to real single-chain magnets

In this section, we are going to show that the selection rules for resonant behaviour in the a.c. susceptibility, experimentally observed in some real molecular chain compounds, are successfully reproduced by our model. The developed formalism is applied to three systems—we know this restriction is far from being exhaustive [1, 3]—namely Mn-, Dy- and Co-based molecular magnetic chains [35, 36, 33]. They were selected, among all representative realizations of SCMs, because a.c. susceptibility data on single crystals are available, which is a fundamental requirement for checking the proposed selection rules. The three systems [35, 36, 33] are characterized by the alternation of two types of magnetic centres along the chain axis so that at least two spins per cell have to be considered; moreover, the magnetic moments are not collinear, the dominant exchange interactions are antiferromagnetic and a strong single-ion anisotropy is present, which favours magnetization alignment along certain crystallographic directions $\hat{\mathbf{z}}_k$. The static properties of these compounds, like magnetization and static susceptibility, are generally well described using a classical Heisenberg model with an isotropic exchange coupling J and a single-ion anisotropy D. Thus, in order to describe the dynamic behaviour in response to a weak, oscillating magnetic field by means of the previously developed theory, it is necessary to relate the Hamiltonian parameters of such a classical spin model to the exchange constant J_I of the effective Ising model (2.2). In the following we will show, through a few examples on real systems, that indeed, depending on the geometry, selection rules are obeyed for the occurrence of slow relaxation of the magnetization at low temperatures ($\beta|J_\mathrm{I}| \gg 1$), as well as for resonant behaviour of the a.c. susceptibility as a function of temperature at low frequencies. As regards the frequencies involved in an a.c. susceptibility experiment on real SCMs, generally [1, 3] they lie in the range 10^{-1}–10^4 Hz, while the attempt frequency α is of the order of 10^9–10^{13} Hz. Thus, for a typical experiment, a resonant peak in the a.c. susceptibility can safely be observed, provided that at least one of the characteristic timescales τ_q involved in (3.3) diverges at low T, in order for the condition (3.8) to be satisfied.

4.1. The Mn^{III}-based single-chain magnet

In the 1D molecular magnetic compound of formula $[Mn(TPP)O_2PPhH]\cdot H_2O$, obtained by reacting Mn(III) acetate *meso*tetraphenylporphyrin with phenylphosphinic acid [35], hereafter denoted by Mn^{III}-based SCM, the phenylphosphinate anion transmits a sizeable antiferromagnetic exchange interaction that, combined with the easy axis magnetic anisotropy of the Mn^{III} sites, gives rise to a canted antiferromagnetic arrangement of the spins. The static single-crystal magnetic properties were analysed in the framework of a classical spin Hamiltonian:

$$\mathcal{H} = -\sum_{r=1}^{N/2}\{J\mathbf{S}_{2r-1}\cdot\mathbf{S}_{2r} + D[(S^{z_1}_{2r-1})^2 + (S^{z_2}_{2r})^2]$$
$$+ \mathrm{e}^{-\mathrm{i}\omega t}\mu_\mathrm{B}H^\alpha g^{\alpha\beta}[S^\beta_{2r-1} + S^\beta_{2r}]\} \qquad (4.1)$$

where $J < 0$ is the antiferromagnetic nearest-neighbour exchange interaction between $S = 2$ spins. $D > 0$ is the uniaxial anisotropy favouring two different local axes, alternating along odd and even sites, respectively; both axes form an angle $\theta = 21.01°$ with the crystallographic c axis, while they form opposite angles of modulus $\phi = 56.55°$ with the a axis (see figure 3). Thus we can write $\hat{\mathbf{z}}_{2r-1} = \sin\theta\cos\phi\hat{\mathbf{e}}_x - \sin\theta\sin\phi\hat{\mathbf{e}}_y + \cos\theta\hat{\mathbf{e}}_z$ and $\hat{\mathbf{z}}_{2r} = \sin\theta\cos\phi\hat{\mathbf{e}}_x + \sin\theta\sin\phi\hat{\mathbf{e}}_y + \cos\theta\hat{\mathbf{e}}_z$.

A best fit of the static single-crystal magnetic susceptibilities, calculated via a Monte Carlo simulation [35], provides $J = -1.34$ K and $D = 4.7$ K; the gyromagnetic tensor $G^{\alpha\beta}$ is diagonal and isotropic with $g^\parallel = 1.97$. Equivalent results can be obtained calculating the static properties of model (4.1) via a transfer matrix approach [41]. Since the uniaxial anisotropy D is rather strong with respect to the exchange coupling $|J|$, as

a first approximation one can assume the two sublattice magnetizations to be directed just along the two easy axes, $\hat{\mathbf{z}}_{2r-1}$ and $\hat{\mathbf{z}}_{2r}$, so that the chain system (4.1) can be described by a non-collinear Ising model formally identical to (2.2), with an effective[3] Ising exchange coupling J_{I} and a generalized Landé factor G_k defined as, respectively

$$J_{\mathrm{I}} = JS(S+1)\cos(\hat{\mathbf{z}}_{2r-1}\cdot\hat{\mathbf{z}}_{2r}),$$
$$G_r = g_r^{\parallel}\sqrt{S(S+1)}\,(\hat{\mathbf{z}}_r\cdot\hat{\mathbf{e}}_H). \tag{4.2}$$

Depending on the orientation of the oscillating magnetic field with respect to the crystallographic axes, the FT of the generalized Landé factor takes the following forms:

$$\tilde{G}_q = g^{\parallel}\sqrt{S(S+1)}\frac{1}{N}\sum_{r=1}^{N/2}\mathrm{e}^{-\mathrm{i}q2r}[\mathrm{e}^{\mathrm{i}q}(\hat{\mathbf{z}}_{2r-1}\cdot\hat{\mathbf{e}}_H)+(\hat{\mathbf{z}}_{2r}\cdot\hat{\mathbf{e}}_H)]$$
$$= g^{\parallel}\sqrt{S(S+1)}$$
$$\times\begin{cases}\sin\theta_1\cos\phi_1\delta_{q,0} & \text{for } H\parallel x\\ \sin\theta_1\sin\phi_1\delta_{q,\pi} & \text{for } H\parallel y\\ \cos\theta_1\delta_{q,0} & \text{for } H\parallel z \text{ (chain axis).}\end{cases} \tag{4.3}$$

The corresponding a.c. susceptibility takes the expression

$$\chi(\omega,T) = N\mu_{\mathrm{B}}^2\beta f(\beta J_{\mathrm{I}})(g^{\parallel})^2[S(S+1)]$$
$$\times\begin{cases}\sin^2\theta\cos^2\phi\dfrac{1}{(1-\gamma_{\mathrm{I}})-\mathrm{i}(\frac{\omega}{\alpha})} & \text{for } H\parallel x\\ \sin^2\theta\sin^2\phi\dfrac{1}{(1+\gamma_{\mathrm{I}})-\mathrm{i}(\frac{\omega}{\alpha})} & \text{for } H\parallel y\\ \cos^2\theta\dfrac{1}{(1-\gamma_{\mathrm{I}})-\mathrm{i}(\frac{\omega}{\alpha})} & \text{for } H\parallel z \text{ (chain axis).}\end{cases} \tag{4.4}$$

Taking into account that, for the Mn^{III} SCM under study, the 'true' exchange coupling, J in (4.1), is antiferromagnetic, and that the angle between the two easy anisotropy axes $\hat{\mathbf{z}}_1$ and $\hat{\mathbf{z}}_2$ is $\delta = 34.6° < 90°$ (see figure 3, right), from (4.2) it follows that the effective Ising exchange coupling is also antiferromagnetic, $J_{\mathrm{I}} < 0$. As a consequence, in the low temperature limit $\beta|J_{\mathrm{I}}| \to \infty$, the relaxation time $\tau_{q=\pi}$ diverges, while $\tau_{q=0}$ does not. Thus, for low frequencies $\omega/\alpha \ll 1$, the a.c. susceptibility presents a resonant behaviour only when the oscillating magnetic field is applied along the crystallographic y axis, i.e. the direction, perpendicular to the chain axis, along which the magnetizations of the two sublattices are *uncompensated* (see figure 3). In contrast, when H is applied parallel to z (the chain axis) or to x, namely two directions along which the magnetizations of the two sublattices are exactly compensated, no resonant behaviour is expected. These theoretical predictions turn out to be in excellent agreement with experimental a.c. susceptibility data [35] obtained in a single-crystal sample of $[Mn(TPP)O_2PPhH]\cdot H_2O$, thus confirming that such a Mn^{III}-based canted antiferromagnet is a *bona fide* SCM.

[3] For a *collinear* Heisenberg ferromagnet with exchange J and anisotropy D, the energy cost of a domain wall was calculated and compared with the energies of a sharp wall and of a soliton: the crossover between the 'sharp wall' regime ($J \ll D$) and the 'broad wall' regime ($J \gg D$) was found to occur [28] for $J/D = 1.8$. In principle, a similar calculation should be performed also for the non-collinear model (4.1), in order to find the limits of validity for the approximation made, e.g. in (4.2).

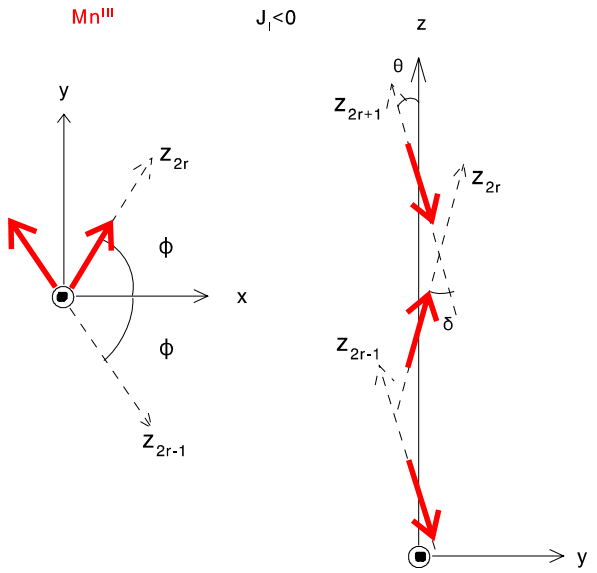

Figure 3. (Colour online) Disposition of local axes ($\hat{\mathbf{z}}_{2r-1}$ and $\hat{\mathbf{z}}_{2r}$) and magnetic moments (red arrows) in the Mn^{III}-based real SCM, discussed in section 4.1, with antiferromagnetic effective Ising exchange coupling $J_{\mathrm{I}} < 0$. Right: schematic view of the chain structure (z is the chain axis) along the crystallographic x axis. Left: projections of local axes (dashed lines) and of magnetic moments (red arrows) in the xy plane, perpendicular to the chain axis.

4.2. *The Dy^{III}-based single-chain magnet*

The molecular magnetic compound of formula $[Dy(hfac)_3(NITPhOPh)]$, hereafter denoted by Dy^{III}-based SCM, belongs to a family of quasi-1D magnets in which rare earth ions (with spin S) and organic radical ions (with spin $s = 1/2$) alternate themselves along the chain axis, z, which in this compound coincides with the crystallographic b axis. Static measurements in single-crystal samples suggest [36, 37] that there is an antiferromagnetic exchange interaction between neighbouring Dy^{III} ions; besides, the easy anisotropy axes of two neighbouring Dy^{III} are canted with respect to the chain axis, and one with respect to each other, in such a way that an uncompensated moment appears along b; the components in the ac plane are, instead, compensated. Thus, as far as the dominant exchange interaction $J < 0$ between Dy^{III} ions is taken into account, the spin Hamiltonian of the system is quite similar to (4.1). However, with respect to the Mn^{III}-based chain, the crystal structure of the Dy^{III}-based SCM is more complicated, not only owing to the presence of two kinds of magnetic centres (the Dy^{III} ions and the organic radical ions), but mainly because the system is formed by two different families of chains, with two almost orthogonal projections of the easy axes in the ac plane, perpendicular to the chain axis: this 'accidental' (in the sense that it is not imposed by symmetry) orthogonality is the reason for the nearly isotropic magnetic behaviour displayed by the system within such a plane [36, 37].

We adopt a simplified model formally equivalent to (4.1). Taking into account only the dominant antiferromagnetic exchange interaction ($J < 0$) between neighbouring Dy^{III} ions (which indeed are next-nearest neighbours in the real system) and their uniaxial anisotropy ($D > 0$), the system can approximately be described by the classical spin Hamiltonian (4.1), where now $|S_k| = 1$. By means of a classical transfer matrix calculation [41], the static properties of the Dy^{III}-based SCM turn out to be satisfactorily fitted [36] by $J = -6$ K, $D = 40$ K, $g^{\parallel} = 10.5$, with the two easy anisotropy axes $\hat{\mathbf{z}}_{2r-1}$, $\hat{\mathbf{z}}_{2r}$ forming equal angles $\theta \approx 75°$ with the chain axis z. (Notice that the latter property holds true for both families of chains.) Also in the case of the Dy^{III}-based SCM, the uniaxial anisotropy D turns out to be sufficiently strong with respect to the exchange coupling $|J|$ in order to assume, as a first approximation (see footnote 3), the two sublattice magnetizations of Dy^{III} to be directed just along the two easy axes. Thus one can define an equivalent non-collinear Ising model (2.2), where the effective Ising exchange coupling J_I and the generalized Landé factor G_r are now defined as

$$J_I = J\cos(\hat{\mathbf{z}}_{2r-1}\cdot\hat{\mathbf{z}}_{2r}), \qquad G_r = g_r^{\parallel}(\hat{\mathbf{z}}_r\cdot\hat{\mathbf{e}}_H). \tag{4.5}$$

Depending on the orientation of the oscillating magnetic field with respect to the crystallographic axes, the FT of the generalized Landé factor takes the form

$$\tilde{G}_q = g^{\parallel}\frac{1}{N}\sum_{r=1}^{N/2} e^{-iq2r}[e^{iq}(\hat{\mathbf{z}}_{2r-1}\cdot\hat{\mathbf{e}}_H)+(\hat{\mathbf{z}}_{2r}\cdot\hat{\mathbf{e}}_H)]$$
$$\propto g^{\parallel}\begin{cases}\cos\theta\ \delta_{q,0} & \text{for } H\parallel z \text{ (chain axis)}\\ \sin\theta\ \delta_{q,\pi} & \text{for } H\perp z.\end{cases} \tag{4.6}$$

It is important to notice that this result holds true for both families (A, B) of chains. Next, we observe that, since in the Dy^{III}-based SCM the spins on opposite sublattices are coplanar with the chain axis, the angle between $\hat{\mathbf{z}}_{2r-1}$ and $\hat{\mathbf{z}}_{2r}$ is just $2\theta \approx 150° > 90°$. Taking into account that the 'true' exchange constant in (4.1) is antiferromagnetic, $J < 0$, from (4.5) it follows that the effective Ising exchange coupling is now ferromagnetic, $J_I > 0$ (see figure 4, top). As a consequence, in the low temperature limit $\beta J_I \to \infty$, the relaxation time $\tau_{q=0}$ diverges, while $\tau_{q=\pi}$ does not. Thus, the a.c. susceptibility

$$\chi(\omega,T) \propto N\mu_B^2\beta f(\beta J_I)(g^{\parallel})^2$$
$$\times\begin{cases}\cos^2\theta\dfrac{1}{(1-\gamma_I)-i(\frac{\omega}{\alpha})} & \text{for } H\parallel z \text{ (chain axis)}\\ \sin^2\theta\dfrac{1}{(1+\gamma_I)-i(\frac{\omega}{\alpha})} & \text{for } H\perp z\end{cases} \tag{4.7}$$

is expected to have a resonant behaviour, for low frequencies $\omega/\alpha \ll 1$, only when the oscillating magnetic field is applied parallel to the chain axis, z, along which the magnetizations of the two sublattices are *uncompensated* (see figure 4, top). Such a theoretical prediction is again in excellent agreement with the experimental a.c. susceptibility data [36] obtained in a single-crystal sample of $[Dy(hfac)_3(NITPhOPh)]_\infty$, thus confirming that the Dy^{III}-based canted antiferromagnet is also a *bona fide* SCM. The only qualitative difference, with respect to the Mn^{III}-based chain, is that, due to the different geometry of the spin

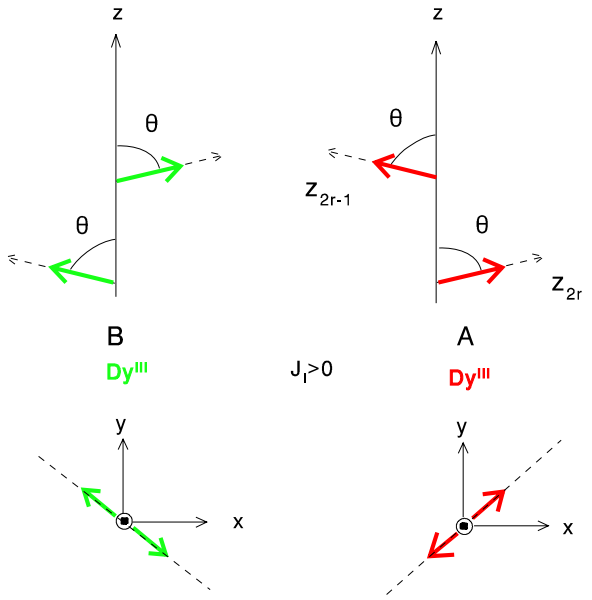

Figure 4. (Colour online) Disposition of odd and even local axes ($\hat{\mathbf{z}}_{2r-1}$ and $\hat{\mathbf{z}}_{2r}$) and magnetic moments (thick arrows) in the Dy^{III}-based real SCM, discussed in section 4.2, with ferromagnetic effective Ising exchange coupling $J_I > 0$. Top: schematic view of the chain structure (z is the chain axis), displaying the two families of chains (A, with red magnetic moments, and B, with green magnetic moments). Bottom: projections of magnetic moments in the xy plane, perpendicular to the chain axis.

arrangement and of the local anisotropy axes with respect to the chain axis, the resonant behaviour of the a.c. susceptibility is now observed for applied field parallel to the chain axis, rather than perpendicular to it.

4.3. The CoPhOMe (Co^{II}-based) single-chain magnet

In the molecular magnetic compound of formula $[Co(hfac)_2$ NITPhOMe], hereafter denoted by CoPhOMe [33, 34], the magnetic contribution is given by cobalt ions, with an Ising character and effective $S = 1/2$, and by NITPhOMe organic radical ions, magnetically isotropic and with $s = 1/2$. The spins are arranged on a helical structure, schematically depicted in figure 5, right, whose projections in a plane perpendicular to the helix axis z (coincident with the crystallographic c axis), are represented in figure 5, left. The primitive magnetic cell is made up of three cobalts (black arrows) and three organic radicals (red arrows). Although the effective spins of the two types of magnetic centres have the same value, the gyromagnetic factors are different: $g_{Co} \neq g_R$; thus, since the nearest-neighbour (cobalt–radical) exchange interaction is negative (and strong, $|J| \approx 100$ K) [34], the sublattice magnetizations are not compensated along z, whereas they are compensated within the xy plane perpendicular to the chain axis z. For this compound, which was the first to display SCM behaviour [33, 34], static measurements on single-crystal samples have not been interpreted in terms of a simple model yet, due to the complexity of the system itself. Thus, a relationship similar to (4.2) and (4.5), which associates the parameters J_I and G_k

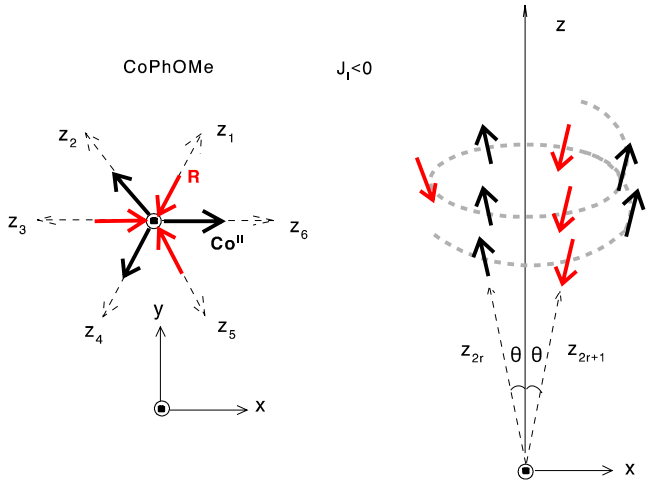

Figure 5. (Colour online) Disposition of even and odd local axes (dashed lines) and magnetic moments (thick arrows) in the CoPhOMe real SCM, discussed in section 4.3, with antiferromagnetic effective Ising exchange coupling $J_{\rm I} < 0$. Right: schematic view of the chain structure (z is the chain axis) along the crystallographic y axis. Left: projections of local axes (dashed lines) and of magnetic moments (thick arrows) in the xy plane, perpendicular to the chain axis.

of the Ising Hamiltonian (2.2) with those of a more realistic Hamiltonian, is still missing. However, the dynamic behaviour has been thoroughly investigated treating—for the sake of simplicity—both the Co^{II} and the organic radical spins as Ising variables, with $\sigma = \pm 1$. The effective Ising Hamiltonian is

$$\mathcal{H} = -\sum_{l=1}^{N/6}\sum_{m=1}^{3}\{J_{\rm I}\sigma_{l,2m}[\sigma_{l,2m-1}+\sigma_{l,2m+1}] + {\rm e}^{-{\rm i}\omega t}\mu_{\rm B}H \times [g_{\rm R}\sigma_{l,2m-1}(\hat{\mathbf{z}}_{2m-1}\cdot\hat{\mathbf{e}}_H) + g_{\rm Co}\sigma_{l,2m}(\hat{\mathbf{z}}_{2m}\cdot\hat{\mathbf{e}}_H)]\} \quad (4.8)$$

where l is the magnetic cell index while m labels odd and even sites, and boundary conditions $\sigma_{l,7} = \sigma_{l+1,1}$ are assumed.

Since all the local axes $\hat{\mathbf{z}}_k$ ($k = 1, \ldots, 6$) form the same angle $\theta \approx 55°$ with the z axis, when a magnetic field is applied along z, the FT of the generalized Landé factor is simply given by

$$\tilde{G}^{\parallel}_q = \cos\theta\frac{1}{N}\sum_{r=1}^{N/2}(g_{\rm Co}{\rm e}^{-{\rm i}q(2r-1)} + g_{\rm R}{\rm e}^{-{\rm i}q2r}) = \frac{\cos\theta}{2}[(g_{\rm Co}+g_{\rm R})\delta_{q,0} + (g_{\rm Co}-g_{\rm R})\delta_{q,\pi}] \quad (4.9)$$

which, except for the prefactor $\cos\theta$, is quite similar to (3.6) for the collinear Ising chain with alternating spins. Thus, the parallel a.c. susceptibility is

$$\chi_{\parallel}(\omega,T) = N\mu_{\rm B}^2\beta f(\beta J_{\rm I})\frac{\cos^2\theta}{4}\left[\frac{(g_{\rm Co}+g_{\rm R})^2}{(1-\gamma_{\rm I}) - {\rm i}(\frac{\omega}{\alpha})} + \frac{(g_{\rm Co}-g_{\rm R})^2}{(1+\gamma_{\rm I}) - {\rm i}(\frac{\omega}{\alpha})}\right]. \quad (4.10)$$

Taking into account that the effective exchange coupling of CoPhOMe is negative ($J_{\rm I} < 0$), the antiferromagnetic branch of the parallel susceptibility is characterized by a diverging timescale $\tau_{q=\pi} = [\alpha(1+\gamma_{\rm I})]^{-1}$ at low temperature so that, for low frequencies $\omega/\alpha \ll 1$, $\chi_{\parallel}(\omega,T)$ displays a resonant behaviour.

Let us now consider the case of a field applied in the plane perpendicular to the chain axis. For $H \parallel x$ (see figure 5, left) one has, letting $k_0 = \frac{\pi}{3}$,

$$G^x_{2r-1} = g_{\rm R}\sin\theta\cos[k_0(2r-1)], \qquad G^x_{2r} = g_{\rm Co}\sin\theta\cos[k_0 2r] \quad (4.11)$$

so that the FT takes the form

$$\begin{aligned}\tilde{G}^x_q &= \sin\theta\frac{1}{N}\sum_{r=1}^{N/2}{\rm e}^{-{\rm i}q2r}\{g_{\rm Co}\cos(k_0 2r) \\ &\quad + g_{\rm R}{\rm e}^{{\rm i}q}[\cos(k_0)\cos(k_0 2r) + \sin(k_0)\sin(k_0 2r)]\} \\ &= \tfrac{1}{4}\sin\theta[(g_{\rm Co}+g_{\rm R}{\rm e}^{{\rm i}(q-k_0)})(\delta_{q,k_0}+\delta_{q,\pi+k_0}) \\ &\quad + (g_{\rm Co}+g_{\rm R}{\rm e}^{{\rm i}(q+k_0)})(\delta_{q,-k_0}+\delta_{q,\pi-k_0})]\end{aligned} \quad (4.12)$$

where, as usual, we have exploited (3.5). Thus it follows that $\tilde{G}_{q=\pm\frac{\pi}{3}} = \frac{\sin\theta}{4}(g_{\rm Co}+g_{\rm R})$ $\tilde{G}_{q=\pi\pm\frac{\pi}{3}} = \frac{\sin\theta}{4}(g_{\rm Co}-g_{\rm R})$.

The corresponding relaxation times are $\tau_{q=\pm\frac{\pi}{3}} = \frac{\alpha}{1-\frac{1}{2}\gamma}$ and $\tau_{q=\pm\frac{2\pi}{3}} = \frac{\alpha}{1+\frac{1}{2}\gamma}$ so that, summing the four contributions we obtain the perpendicular a.c. susceptibility:

$$\chi_{\perp}(\omega,T) = N\mu_{\rm B}^2\beta f(\beta J_{\rm I})\frac{\sin^2\theta}{8} \times \left[\frac{(g_{\rm Co}+g_{\rm R})^2}{(1-\frac{1}{2}\gamma) - {\rm i}(\frac{\omega}{\alpha})} + \frac{(g_{\rm Co}-g_{\rm R})^2}{(1+\frac{1}{2}\gamma) - {\rm i}(\frac{\omega}{\alpha})}\right]. \quad (4.13)$$

In conclusion, for the sixfold helix model with alternating spins and Ising exchange coupling in (4.8), the parallel and perpendicular components of the a.c. susceptibility, $\chi_{\parallel}(\omega,T)$ and $\chi_{\perp}(\omega,T)$, display a behaviour similar to that of a ferrimagnetic chain with alternating spins (see (3.7)) and of an n-fold helical spin arrangement with equivalent spins (see (B.4)), respectively. In spite of the approximations involved in model (4.8) to describe the real CoPhOMe molecular magnetic chain, the two calculated susceptibilities (4.10) and (4.13) qualitatively reproduce the dynamic behaviour of this compound [33, 34]. In fact, no out-of-phase a.c. susceptibility (imaginary part) is observed when the field is applied in the plane perpendicular to the chain axis, z, for the experimental frequencies (1–10^5 Hz) [34]. This confirms the general result derived in appendix B that forbids the observation of a resonant behaviour in $\chi_{\perp}$ for an Ising spin chain arranged as an n-fold helix with $n > 2$. In contrast, when the oscillating field is parallel to z, a resonant behaviour is observed as a function of temperature. Even though our theoretical treatment holds only for small deviations from equilibrium, it is worth mentioning that the absence of slow relaxation for fields applied in the perpendicular plane is shown in the low temperature magnetization curve as well: at low enough temperatures, a finite-area hysteresis loop (of dynamic origin) is present only when a static field is applied parallel to the chain axis, while no hysteresis is observed in the in-plane magnetization curve [33, 34].

4.4. Slow versus fast relaxation of the spontaneous magnetization

We conclude this section, devoted to comparison with experimental systems, mentioning what our simple model

would predict for the relaxation, after field removal, in collinear ferro- and ferrimagnetic chains. The following considerations are based on realistic values for the exchange coupling in real SCMs and accessible magnetic fields. However, since relaxation is a strongly out-of-equilibrium process, predictions in this context are not expected to be as reliable as the selection rules derived for a.c. susceptibility; in fact, only small departures from equilibrium are assumed in the present theory.

In appendix C, the time evolution of $s_k(t)$ starting from two physically meaningful initial conditions is derived, showing that spins located on the even and odd sites of a linear lattice relax from saturation following a mono-exponential law (see (C.11) and (C.12)). Different characteristic timescales, $\tau_{q=0}$ and $\tau_{q=\pi}$, are found depending on whether an initial condition of full or partial saturation is assumed ((C.1) and (C.2), respectively). As a consequence, the macroscopic magnetization, expressed by (2.4), also displays the same mono-exponential relaxation as the single-site quantities $s_k(t)$. Limiting our analysis to collinear spin chains, the case in which all the magnetic moments are equal ($g_e = g_o$) and the case in which two sublattices are present ($g_e \neq g_o$) display a different physical scenario and need to be discussed separately.

- For $g_e = g_o$, a spin chain can only be prepared in the saturated initial configuration (C.1), with all the spins aligned in the same direction, through the application of an external field so that the corresponding relaxation time is $\tau_{q=0}$ (see (C.11)). Thus, when the field is abruptly removed, such a system is expected to relax slowly at low temperature only if the exchange coupling is ferromagnetic ($J_I > 0$). In contrast, if the exchange coupling is antiferromagnetic ($J_I < 0$) and the chain is 'forced' in the saturated state by a strong applied magnetic field, the system is expected to relax very fast (in a typical time of the order of α^{-1}) when the field is removed.
- As pointed out in section 1, a model with antiferromagnetic coupling ($J_I < 0$) but non-compensated magnetic moments on the two sublattices ($g_e \neq g_o$) is more akin to real SCMs [1, 3, 33]. Yet it is very interesting since, depending on the intensity of the applied magnetic field, the system can be prepared either in the saturated initial configuration (C.1), where all spins are parallel to each other, or in the partially saturated one (C.2), where nearest neighbours are antiparallel. In the former case, a very strong field is required in order to overcome the antiferromagnetic coupling between nearest neighbours; once the field is removed, the relaxation of the magnetization is expected to be fast at low temperatures, on the basis of the solution (C.11). In the latter case, the partially saturated initial configuration (C.2) can easily be obtained through the application of a smaller, experimentally accessible magnetic field; when the field is abruptly removed, the relaxation is expected to be slow according to the solution (C.12). The solution (C.12) justifies the observation of hysteretical behaviour of dynamic origin in ferrimagnetic quasi-1D compounds like CoPhOMe [33].

Summarizing, according to Glauber dynamics, when a collinear ferrimagnetic chain is prepared in an initial state—fully or partially saturated depending on the intensity of the applied magnetic field—once the field is removed abruptly, the spin system can show fast or slow relaxation, respectively. Fast relaxation corresponds to stronger fields. Due to its large antiferromagnetic exchange constant ($|J_I| \sim 100$ K) [33, 34], preparing the CoPhOMe molecular chain in the fully saturated initial configuration would require very high, almost inaccessible, fields (∼1000 kOe). Thus this compound is not a good candidate for such kinds of experiments.

5. Conclusions

In conclusion, in the framework of a one-dimensional Ising model with single spin-flip Glauber dynamics, taking into account non-collinearity of local anisotropy axes between themselves and with respect to the crystallographic (laboratory) frame, we have investigated: (i) the dynamics of magnetization reversal in zero field and (ii) the response of the system to a weak magnetic field, oscillating in time. We have shown that SCM behaviour is not only a feature of collinear ferro- and ferrimagnetic, but also of canted antiferromagnetic, chains. In particular, we have found that resonant behaviour of the a.c. susceptibility versus temperature in response to an oscillating magnetic field is possible, at low frequency, only for fields applied in a direction where magnetic moments are uncompensated. In contrast, a broad peak is expected when there is no net magnetization along the field direction.

The role played by geometry in selecting the timescales involved in a process is an important and peculiar result, typical of a magneto-molecular approach to low-dimensional magnetism. In fact, magnetic centres with uniaxial anisotropy usually correspond to building blocks with low symmetry [42, 43], which—in turn—often crystallize in more symmetric space groups, realizing a reciprocal non-collinearity between local anisotropy axes as a natural consequence [1, 2]. Thus the family of real SCMs, to which our model applies, does not restrict to ad hoc synthesized compounds but, instead, is expected to grow larger in the future [3]. As a validity check of our selection rules (as well as a tutorial exemplification), we have shown how our theory applies successfully to three different molecular-based spin chains; when possible, we have put the parameters of our model Hamiltonian (2.2) in relationship with those of more general models, typically used to fit the static properties of the corresponding compounds. Needless to say, the possibility of schematizing the chosen three compounds with Hamiltonian (2.2) relies on the fact that at low enough temperatures they behave as chains consisting of two-level units coupled by a fully anisotropic exchange interaction. The latter assumption is expected to hold also for spin larger than one-half in the presence of strong single-ion anisotropy, provided that domain walls still remain sharp [28] (see footnote 3). In this case each single magnetic centre follows a thermally activated dynamics, with an energy barrier Δ_0, and well-established heuristic arguments [44] suggested to replace the attempt frequency by $\alpha = \alpha_0 e^{-\beta\Delta_0}$.

A naive application of our threefold-helix results (B.3) and (B.4) to the recently synthesized non-collinear Dy_3 cluster

would prevent the observation of *slow* relaxation, while single-molecule-magnet dynamics is indeed observed there even in the presence of compensated magnetic moments [45]. However, such a behaviour in the classical regime, i.e. far from level crossings where underbarrier processes of quantum origin are important, is observed for Dy_3 in non-zero field and the resonant behaviour is due to a change of the relative population between the lowest and the first excited Kramers doublets of each Dy ion: for sure, this mechanism cannot be accounted for when dealing with two-level elementary variables, like σ_k in Hamiltonian (2.2). An extension of our model to multivalued σ_ks definitely deserves to be considered in the future.

Beyond molecular spin chains, our approach might also be used to model monatomic nanowires showing slow relaxation of the magnetization at low temperatures [46] and, possibly, one-dimensional spin glasses [47] (provided that quenched disorder is somehow taken into account). In this regard, the question of distinguishing between SCM and spin-glass behaviour in quasi-1D systems is still a hot topic of discussion [48–51].

After the successful organization of single-molecule magnets onto surfaces [52–54], the grafting of properly functionalized SCMs on substrates represents a foreseeable goal as well as a fundamental step for their possible use as magnetic-memory units [3]. Technologies employing more traditional materials, but based on alternative geometrical arrangements of magnetic anisotropy axes with respect to the switching field, such as in perpendicular recording [55] or processional switching [56], are already at the stage of forthcoming implementation in devices. Were SCMs to be considered as a possible route to tackle the main issues of high-density magnetic storage—i.e. optimization of the signal–noise ratio, thermal stability and writeability [55]—the proposed selection rules for slow relaxation, and related bistability, might find an application in magnetic-memory manufacture as well.

Acknowledgments

We wish to thank R Sessoli and A Rettori for stimulating discussions, and J Villain for interest and fruitful suggestions in the early stages of this research work. Financial support from ETHZ, the Swiss National Foundation and Italian CNR is also acknowledged.

Appendix A. The a.c. susceptibility of a non-collinear Ising chain

For weak applied a.c. fields, δ_k can be linearized:

$$\delta_k = \tanh(\beta\mu_B G_k H(t)) \approx \beta\mu_B G_k H(t) \tag{A.1}$$

so that the system of equations of motion (3.1) takes the form

$$\frac{\mathrm{d}s_k(t)}{\mathrm{d}(\alpha t)} = -s_k(t) + \frac{\gamma}{2}[s_{k+1}(t) + s_{k-1}(t)] \tag{A.2}$$

where

$$f(\beta J_I) = 1 - \gamma\eta = \frac{1-\eta^2}{1+\eta^2} \tag{A.3}$$

is a function of the reduced coupling constant βJ_I and we have taken into account that $\gamma = 2\eta/(1+\eta^2)$. After a brief transient period, the system will reach the stationary condition in which the magnetic moment of each spin oscillates coherently with the forcing term at the frequency ω. The expectation value of a spin on the kth lattice site, $s_k(t)$, can be expressed through its spatial FT, $\tilde{s}_q$, which leads to the trial solution

$$s_k(t) = \sum_q \tilde{s}_q \mathrm{e}^{\mathrm{i}qk}\,\mathrm{e}^{-\mathrm{i}\omega t}. \tag{A.4}$$

By substituting the latter in the system (A.2) we get

$$\tilde{s}_q = \beta f(\beta J_I)\mu_B H \frac{\alpha\tilde{G}_q}{\alpha(1-\gamma\cos q) - \mathrm{i}\omega}, \tag{A.5}$$

where $\tilde{G}_q$ is the FT of G_k:

$$\tilde{G}_q = \frac{1}{N}\sum_{k=1}^{N} \mathrm{e}^{-\mathrm{i}qk} G_k. \tag{A.6}$$

The average of stochastic magnetization can readily be obtained from (2.4) as

$$\langle M\rangle_t = \mu_B \mathrm{e}^{-\mathrm{i}\omega t} \sum_{k=1}^{N}\sum_{qq'} \tilde{G}_q \tilde{s}_{q'} \mathrm{e}^{\mathrm{i}qk}\,\mathrm{e}^{\mathrm{i}q'k}, \tag{A.7}$$

which accounts for non-collinearity of local anisotropy axes with respect to the field direction. The summation over all the lattice sites (k indices) yields a factor $N\delta_{q,-q'}$ in (A.7); substituting the expression (A.5) for $\tilde{s}_q$, one obtains

$$\langle M\rangle_t = N\mu_B^2 \beta f(\beta J_I) H \mathrm{e}^{-\mathrm{i}\omega t} \sum_{qq'} \frac{\alpha\tilde{G}_q\tilde{G}_{q'}\delta_{q,-q'}}{\alpha(1-\gamma\cos q) - \mathrm{i}\omega}. \tag{A.8}$$

The a.c. susceptibility is finally obtained by dividing (A.8) by $H\mathrm{e}^{-\mathrm{i}\omega t}$:

$$\chi(\omega, T) = N\mu_B^2 \beta f(\beta J_I) \sum_q \frac{\alpha|\tilde{G}_q|^2}{\alpha(1-\gamma\cos q) - \mathrm{i}\omega} \tag{A.9}$$

(where $\tilde{G}_q\tilde{G}_{-q} = |\tilde{G}_q|^2$).

Appendix B. The a.c. susceptibility of an *n*-fold helix

As an example of a non-collinear spin arrangement, we consider a system of spins with the local axes of anisotropy arranged on an n-fold helix (see figure B.1); θ is the angle that the local axes form with z, the unique axis of the helix (i.e. the chain axis). In this case the Landé factors are equal on all lattice sites, but different spins experience different fields because of the geometrical arrangement of magnetic moments. In the following we will make the approximation that the Landé tensor of a spin on the kth lattice site has just a non-zero component g along the easy anisotropy direction $\hat{\mathbf{z}}_k$, so that $G_k = g\hat{\mathbf{z}}_k \cdot \hat{\mathbf{e}}_H$ (see (2.3)). In the crystallographic frame (x, y, z), the directors $\hat{\mathbf{z}}_k$ are (integer k)

$$\hat{\mathbf{z}}_k = \sin\theta\left[\cos\left(\frac{2\pi k}{n}\right)\hat{\mathbf{e}}_x + \sin\left(\frac{2\pi k}{n}\right)\hat{\mathbf{e}}_y\right] + \cos\theta\hat{\mathbf{e}}_z. \tag{B.1}$$

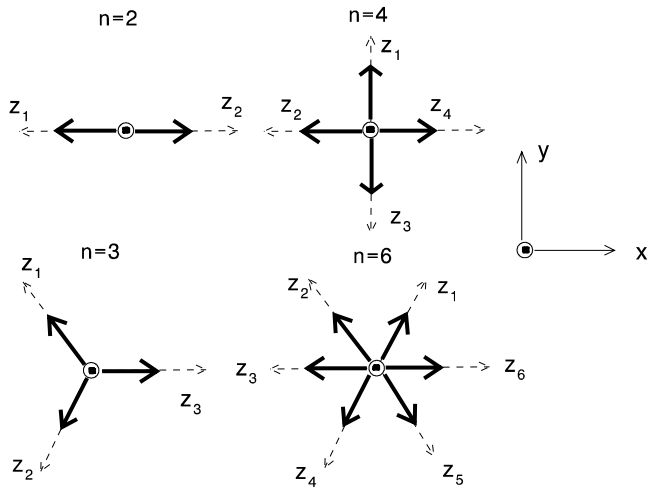

Figure B.1. Thick arrows denote the projections on the xy plane, perpendicular to the chain (helix) axis z, of magnetic moments in a one-dimensional Ising helimagnet, for different fold symmetries ($n = 2, 3, 4, 6$). Dashed lines are the projections of the local axes of anisotropy, $\hat{\mathbf{z}}_k$.

Let us first consider the case of an oscillating magnetic field H applied parallel to z, the helix axis. All the spins actually undergo the same field, and since $G_k = g\cos\theta$ independently of the lattice site k, the only peak in the FT $\tilde{G}_q$ occurs at $q = 0$:

$$\tilde{G}^z_q = g\cos\theta\,\delta_{q,0}\ (\forall\, n). \tag{B.2}$$

Following the same procedure as in section 3.1, the parallel a.c. susceptibility ($\parallel = zz$) takes the form

$$\chi_\parallel(\omega, T) = N\mu_B^2\beta f(\beta J_I)\frac{g^2\cos^2\theta}{(1-\gamma) - \mathrm{i}(\frac{\omega}{\alpha})}\ (\forall\, n) \tag{B.3}$$

which is valid for any value of the helix fold index n. A resonant behaviour is expected in this case for $J_I > 0$.

Now we consider the case of an oscillating field H applied perpendicularly to the chain axis with $n > 2$.

- $n > 2$. In this case, denoting by $\hat{\mathbf{e}}_x \cdot \hat{\mathbf{e}}_H$ and $\hat{\mathbf{e}}_y \cdot \hat{\mathbf{e}}_H$ the directors of the in-plane field, the FTs of G_k are given by

$$\begin{aligned}\tilde{G}^x_q &= \frac{1}{N}(\hat{\mathbf{e}}_x \cdot \hat{\mathbf{e}}_H)g\sin\theta\sum_{k=1}^{N}\cos\Big(\frac{2\pi k}{n}\Big)\mathrm{e}^{-\mathrm{i}qk}\\ &= (\hat{\mathbf{e}}_x \cdot \hat{\mathbf{e}}_H)g\sin\theta\tfrac{1}{2}(\delta_{q,\frac{2\pi}{n}} + \delta_{q,-\frac{2\pi}{n}})\\ \tilde{G}^y_q &= \frac{1}{N}(\hat{\mathbf{e}}_y \cdot \hat{\mathbf{e}}_H)g\sin\theta\sum_{k=1}^{N}\sin\Big(\frac{2\pi k}{n}\Big)\mathrm{e}^{-\mathrm{i}qk}\\ &= (\hat{\mathbf{e}}_y \cdot \hat{\mathbf{e}}_H)g\sin\theta\frac{1}{2\mathrm{i}}(\delta_{q,\frac{2\pi}{n}} - \delta_{q,-\frac{2\pi}{n}}).\end{aligned}$$

Remarkably, just as $|\tilde{G}_q|^2$ appears in (3.3), the general result for the in-plane susceptibility turns out to be independent of the field direction. Thus, for $n > 2$, the perpendicular ($\perp$) a.c. susceptibility of the n-fold helix is given by

$$\chi_\perp(\omega, T) = N\mu_B^2\beta f(\beta J_I)\tfrac{1}{2}\sin^2\theta \times \frac{g^2}{[1-\gamma\cos(\frac{2\pi}{n})] - \mathrm{i}(\frac{\omega}{\alpha})}, \tag{B.4}$$

where we have exploited the fact that $\cos(-\frac{2\pi}{n}) = \cos(\frac{2\pi}{n})$ for the term appearing at the denominator of (3.3).

Note that a resonant behaviour is *never* expected—neither for $J_I > 0$ nor for $J_I < 0$—when the a.c. field is applied perpendicularly to an n-fold helix with $n > 2$.

Appendix C. Relaxation of the magnetization in zero field

The original Glauber model was formulated for a chain of collinear spins with the same Landé factors [6]: i.e. in (2.2) one has $G_k = g, \forall\, k = 1, \ldots, N$. Assuming that the system has been fully magnetized by means of a strong external field, one can study how the system evolves if the field is removed abruptly. This corresponds to taking a fully saturated initial condition

$$s_k(0) = 1, \quad \forall\, k. \tag{C.1}$$

The configuration with all the spins aligned in the same direction (C.1) reflects an experimental situation that can be easily obtained for ferromagnetic coupling ($J_I > 0$) but may require very strong fields (possibly inaccessible) for antiferromagnetic couplings ($J_I < 0$).

In ferrimagnetic chains, on the other hand, a 'partial' saturation can be reached, provided the antiferromagnetic coupling ($J_I < 0$) between nearest neighbours is 'strong enough', meaning that the antiferromagnetic coupling must be much larger ($J_I \approx$ 100–1000 K) than the Zeeman energy associated with accessible magnetic fields (as often happens in experiments [1, 3]). In fact, if the Landé factors for odd and even sites are not equal ($g_o \neq g_e$), through the application of an opportune field the sample can be prepared in a configuration with

$$s_k(0) = \begin{cases} +1 & \text{for } k = 2r+1\ (k \text{ odd})\\ -1 & \text{for } k = 2r\ (k \text{ even}).\end{cases} \tag{C.2}$$

With respect to the case considered by Glauber, it is convenient to separate explicitly the expectation values of the odd sites, $s_{2r+1}(t)$, from those of the even sites, $s_{2r}(t)$. Thus, for $H = 0$, the set of N equations of motion (2.9) can be rewritten as

$$\begin{aligned}\frac{\mathrm{d}}{\mathrm{d}t}s_{2r} &= -\alpha\big[s_{2r} + \tfrac{1}{2}\gamma(s_{2r+1} + s_{2r-1})\big]\\ \frac{\mathrm{d}}{\mathrm{d}t}s_{2r+1} &= -\alpha\big[s_{2r+1} + \tfrac{1}{2}\gamma(s_{2r} + s_{2r-2})\big].\end{aligned} \tag{C.3}$$

In the following, the solutions of (C.3) will be found using two different approaches that yield identical results.

C.1. The generating function approach

First, we expose in detail the generating function approach that closely follows Glauber's original paper. By assuming periodic boundary conditions and defining the two generating functions:

$$\begin{aligned}\mathcal{L}(y,t) &= \sum_{r=-\infty}^{+\infty} y^{2r+1}\, s_{2r+1}(t),\\ \mathcal{G}(y,t) &= \sum_{r=-\infty}^{+\infty} y^{2r}\, s_{2r}(t),\end{aligned} \tag{C.4}$$

(C.3) can be expressed as two differential equations:

$$\begin{aligned}\dot{\mathcal{L}}(y,t) &= -\mathcal{L}(y,t) + \tfrac{1}{2}\gamma(y+y^{-1})\mathcal{G}(y,t)\\ \dot{\mathcal{G}}(y,t) &= -\mathcal{G}(y,t) + \tfrac{1}{2}\gamma(y+y^{-1})\mathcal{L}(y,t)\end{aligned} \tag{C.5}$$

(with the dot indicating the first derivative with respect to the adimensional variable αt). The system (C.5) can be decoupled through the substitution

$$\begin{aligned}\mathcal{U}(y,t) &= \mathcal{L}(y,t) + \mathcal{G}(y,t),\\ \mathcal{W}(y,t) &= \mathcal{L}(y,t) - \mathcal{G}(y,t),\end{aligned} \tag{C.6}$$

from which it follows

$$\dot{\mathcal{U}}(y,t) = -(1-\nu)\mathcal{U}(y,t)$$

$$\dot{\mathcal{W}}(y,t) = -(1+\nu)\mathcal{W}(y,t),$$

with $\nu = \frac{1}{2}\gamma(y+y^{-1})$. The solutions of these two equations are $\mathcal{U}(y,t) = \mathcal{U}(y,0)\mathrm{e}^{-(1-\nu)\alpha t}$ and $\mathcal{W}(y,t) = \mathcal{W}(y,0)\mathrm{e}^{-(1+\nu)\alpha t}$ and, exploiting the property

$$\exp\left[\tfrac{1}{2}(y+y^{-1})x\right] = \sum_{k=-\infty}^{+\infty} y^k\,\mathcal{I}_k(x) \tag{C.7}$$

of the Bessel functions of imaginary argument $\mathcal{I}_k(x)$, can be rewritten as

$$\mathcal{U}(y,t) = \mathcal{U}(y,0)\mathrm{e}^{-\alpha t}\sum_{k=-\infty}^{+\infty} y^k\mathcal{I}_k(\gamma\alpha t)$$

$$\mathcal{W}(y,t) = \mathcal{W}(y,0)\mathrm{e}^{-\alpha t}\sum_{k=-\infty}^{+\infty} (-1)^k y^k\mathcal{I}_k(\gamma\alpha t).$$

The solutions to the system (C.5) can be obtained from the inverse transformation of (C.6):

$$\begin{aligned}\mathcal{L}(y,t) &= \tfrac{1}{2}\mathrm{e}^{-\alpha t}\sum_{k=-\infty}^{+\infty} y^k\,[\mathcal{U}(y,0)\mathcal{I}_k(\gamma\alpha t)\\ &\quad + (-1)^k\mathcal{W}(y,0)\mathcal{I}_k(\gamma\alpha t)]\\ \mathcal{G}(y,t) &= \tfrac{1}{2}\mathrm{e}^{-\alpha t}\sum_{k=-\infty}^{+\infty} y^k\,[\mathcal{U}(y,0)\mathcal{I}_k(\gamma\alpha t)\\ &\quad - (-1)^k\mathcal{W}(y,0)\mathcal{I}_k(\gamma\alpha t)].\end{aligned}$$

Then, separating the k-odd from the k-even terms in both sums, one gets

$$\begin{aligned}\mathcal{L}(y,t) &= \mathrm{e}^{-\alpha t}\sum_{r=-\infty}^{+\infty}[y^{2r}\mathcal{L}(y,0)\mathcal{I}_{2r}(\gamma\alpha t)\\ &\quad + y^{2r+1}\mathcal{G}(y,0)\mathcal{I}_{2r+1}(\gamma\alpha t)]\\ \mathcal{G}(y,t) &= \mathrm{e}^{-\alpha t}\sum_{r=-\infty}^{+\infty}[y^{2r}\mathcal{G}(y,0)\mathcal{I}_{2r}(\gamma\alpha t)\\ &\quad + y^{2r-1}\mathcal{L}(y,0)\mathcal{I}_{2r-1}(\gamma\alpha t)].\end{aligned}$$

By means of (C.4), the functions $\mathcal{L}(y,0)$ and $\mathcal{G}(y,0)$ can be expressed in terms of the initial single-spin expectation values, $s_{2r}(0)$ and $s_{2r+1}(0)$ respectively, so that

$$\begin{aligned}\mathcal{L}(y,t) &= \mathrm{e}^{-\alpha t}\sum_{r=-\infty}^{+\infty}\Bigg[y^{2r}\sum_{m=-\infty}^{+\infty} y^{2m+1}s_{2m+1}(0)\mathcal{I}_{2r}(\gamma\alpha t)\\ &\quad + y^{2r+1}\sum_{m=-\infty}^{+\infty} y^{2m}s_{2m}(0)\mathcal{I}_{2r+1}(\gamma\alpha t)\Bigg].\end{aligned}$$

Putting $k' = k+m$ we have

$$\begin{aligned}\mathcal{L}(y,t) &= \mathrm{e}^{-\alpha t}\sum_{k'=-\infty}^{+\infty} y^{2k'+1}\sum_{m=-\infty}^{+\infty}[s_{2m+1}(0)\mathcal{I}_{2(k'-m)}(\gamma\alpha t)\\ &\quad + s_{2m}(0)\mathcal{I}_{2(k'-m)+1}(\gamma\alpha t)].\end{aligned} \tag{C.8}$$

By comparing this latter result with the definition of $\mathcal{L}(y,t)$ (C.4) and requiring that the terms corresponding to the same power of y be equal, an explicit function for the odd-spin expectation values is readily obtained:

$$\begin{aligned}s_{2r+1}(t) &= \mathrm{e}^{-\alpha t}\sum_{m=-\infty}^{+\infty}[s_{2m+1}(0)\mathcal{I}_{2(r-m)}(\gamma\alpha t)\\ &\quad + s_{2m}(0)\mathcal{I}_{2(r-m)+1}(\gamma\alpha t)].\end{aligned} \tag{C.9}$$

The substitution of $\mathcal{L}(y,0)$ and $\mathcal{G}(y,0)$ in the solution found for $\mathcal{G}(y,t)$ yields, after analogous passages, the expectation value for even sites:

$$\begin{aligned}s_{2r}(t) &= \mathrm{e}^{-\alpha t}\sum_{m=-\infty}^{+\infty}[s_{2m}(0)\mathcal{I}_{2(r-m)}(\gamma\alpha t)\\ &\quad + s_{2m+1}(0)\mathcal{I}_{2(r-m)-1}(\gamma\alpha t)].\end{aligned} \tag{C.10}$$

In order to distinguish between the ferromagnetic and ferrimagnetic relaxations, we specialize the general solutions, (C.9) and (C.10) to the two different kinds of initial conditions (C.1) and (C.2). In both cases, we will assume that the exchange coupling J_{I} is negative.

Let us start from the saturated configuration (C.1), and substitute the initial condition $s_k(0) = 1$ for all k in both (C.9) and (C.10):

$$s_{2r}(t) = \mathrm{e}^{-\alpha t}\sum_{m=-\infty}^{+\infty}[\mathcal{I}_{2(r-m)}(\gamma\alpha t) + \mathcal{I}_{2(r-m)-1}(\gamma\alpha t)]$$

$$s_{2r+1}(t) = \mathrm{e}^{-\alpha t}\sum_{m=-\infty}^{+\infty}[\mathcal{I}_{2(r-m)}(\gamma\alpha t) + \mathcal{I}_{2(r-m)+1}(\gamma\alpha t)].$$

Hence, by exploiting the property (C.7) of the Bessel functions (taking $y = 1$), and redefining the sums by a unique index j, we get

$$\begin{aligned}s_{2r}(t) &= \mathrm{e}^{-\alpha t}\sum_{j=-\infty}^{+\infty}\mathcal{I}_j(\gamma\alpha t) = \mathrm{e}^{-\alpha(1-\gamma)t}\\ s_{2r+1}(t) &= \mathrm{e}^{-\alpha t}\sum_{j=-\infty}^{+\infty}\mathcal{I}_j(\gamma\alpha t) = \mathrm{e}^{-\alpha(1-\gamma)t}.\end{aligned} \tag{C.11}$$

This result tells that, starting with all the spins aligned in the same direction, the expectation value of each spin (both on even and odd sites) decays as a mono-exponential law with relaxation time $\tau_{q=0} = [\alpha(1-\gamma)]^{-1}$, which is just the characteristic timescale obtained as the inverse of the dispersion relation λ_q with zero wavenumber $q = 0$ (see (2.11)). Notice that $\tau_{q=0}$ can diverge for $T \to 0$ only in the case of ferromagnetic coupling, $J_{\mathrm{I}} > 0$ ($\gamma > 0$).

Let us now consider the partially saturated configuration (C.2), in which $s_k(0) = 1$ for k odd and $s_k(0) = -1$ for k even. (C.9) and (C.10) specialized to those initial conditions are

$$s_{2r}(t) = -\mathrm{e}^{-\alpha t}\sum_{m=-\infty}^{+\infty}[\mathcal{I}_{2(r-m)}(\gamma\alpha t) - \mathcal{I}_{2(r-m)-1}(\gamma\alpha t)]$$

$$s_{2r+1}(t) = \mathrm{e}^{-\alpha t} \sum_{m=-\infty}^{+\infty} [\mathcal{I}_{2(r-m)}(\gamma\alpha t) - \mathcal{I}_{2(r-m)+1}(\gamma\alpha t)]\,;$$

again from the property (C.7) (but now for $y = -1$), it follows

$$\begin{aligned} s_{2r}(t) &= -\mathrm{e}^{-\alpha t} \sum_{j=-\infty}^{+\infty} (-1)^j \mathcal{I}_j(\gamma\alpha t) = -\mathrm{e}^{-\alpha(1+\gamma)t} \\ s_{2r+1}(t) &= \mathrm{e}^{-\alpha t} \sum_{j=-\infty}^{+\infty} (-1)^j \mathcal{I}_j(\gamma\alpha t) = \mathrm{e}^{-\alpha(1+\gamma)t}. \end{aligned} \tag{C.12}$$

Also in this case all the spins of the system relax with a mono-exponential law, but now the relaxation time is $\tau_{q=\pi} = [\alpha(1+\gamma)]^{-1}$, which corresponds to the inverse of the eigenvalue λ_q with wavenumber $q = \pi$, see (2.11). Notice that $\tau_{q=\pi}$ can diverge for $T \to 0$ only in the case of antiferromagnetic coupling, $J_\mathrm{I} < 0$ ($\gamma < 0$).

Summarizing, according to the sign of the exchange constant, both timescales $\tau_{q=0}$ (for $J_\mathrm{I} > 0$) and $\tau_{q=\pi}$ (for $J_\mathrm{I} < 0$) diverge in the low temperature limit $T \to 0$, following an Arrhenius law:

$$\tau = \frac{1}{2\alpha} \mathrm{e}^{4\beta|J_I|} \tag{C.13}$$

with energy barrier $4|J_\mathrm{I}|$ (slow relaxing mode). It is worth noting that the remaining relaxation times, given by the inverse of the eigenvalues in (2.11) with $q \neq 0$ and π, always remain of the same order of magnitude as α^{-1} (fast relaxing modes). This timescale is typically very small (∼ps) in real systems, and negligible with respect to the characteristic times involved in any experimental measurement we refer to.

C.2. The Fourier transform approach

The solutions, (C.11) and (C.12), to the set of equations (C.3) can alternatively be deduced within the Fourier transform (FT) formalism, which has already been exploited to obtain the dispersion relation (2.11). Recalling the definition (2.10) of $s_k(t)$ and its spatial FT:

$$\tilde{s}_q = \frac{1}{N} \sum_k s_k(t) \mathrm{e}^{-\mathrm{i}qk}\, \mathrm{e}^{\lambda_q t}, \tag{C.14}$$

we evaluate $\tilde{s}_q$ at time $t = 0$, $\tilde{s}_q = \frac{1}{N}\sum_k s_k(0)\mathrm{e}^{-\mathrm{i}qk}$, for the two initial conditions of interest (C.1) and (C.2). Starting from the all-spin-up configuration (C.1), we have

$$\tilde{s}_q = \frac{1}{N} \sum_k \mathrm{e}^{-\mathrm{i}qk} = \delta_{q,0}. \tag{C.15}$$

Hence, the solution for the expectation value of a spin localized on the k lattice site at time t is

$$s_k(t) = \sum_q \delta_{q,0} \mathrm{e}^{\mathrm{i}qk} \mathrm{e}^{-\lambda_q t} = \mathrm{e}^{-\lambda_{q=0} t}, \tag{C.16}$$

which is identical to (C.11) since $\lambda_{q=0} = \alpha(1-\gamma)$.

Starting from the partially saturated configuration (C.2), it is useful to rewrite it as $s_k(0) = -\mathrm{e}^{\mathrm{i}\pi k}$, so that the FT at $t = 0$ is

$$\tilde{s}_q = -\frac{1}{N} \sum_k \mathrm{e}^{\mathrm{i}\pi k}\, \mathrm{e}^{-\mathrm{i}qk} = -\delta_{q,\pi}. \tag{C.17}$$

Hence, the solution is readily obtained:

$$s_k(t) = -\sum_q \delta_{q,\pi} \mathrm{e}^{\mathrm{i}qk}\, \mathrm{e}^{-\lambda_q t} = -\mathrm{e}^{\mathrm{i}\pi k} \mathrm{e}^{-\lambda_{q=\pi} t}, \tag{C.18}$$

which is identical to (C.12) since $\lambda_{q=\pi} = \alpha(1+\gamma)$.

Finally, we observe that (C.16) and (C.18) hold even for a ring with a *finite* number N of spins, while (C.11) and (C.12) were obtained in the infinite-chain limit.

References

[1] Coulon C, Miyasaka H and Clérac R 2006 *Struct. Bond.* **122** 163 and references therein
[2] Miyasaka H and Yamashita M 2007 *Dalton Trans.* **399** and references therein
[3] Bogani L, Vindigni A, Sessoli R and Gatteschi D 2008 *J. Mater. Chem.* **18** 4750 and references therein
[4] Braun H B 1993 *Phys. Rev. Lett.* **71** 3557
[5] Braun H B 1999 *J. Appl. Phys.* **85** 6172 and references therein
[6] Glauber R J 1963 *J. Math. Phys.* **4** 294
[7] Anderson J E 1969 *J. Chem. Phys.* **52** 2021
[8] Bozdemir S 1980 *Phys. Status Solidi* b **104** 37
[9] Bozdemir S 1981 *Phys. Status Solidi* b **103** 459
[10] Skinner J L 1983 *J. Chem. Phys.* **79** 1955
[11] Berim G O and Ruckenstein E 2003 *J. Chem. Phys.* **119** 9640
[12] Brey J J and Prados A 1996 *Phys. Rev.* E **53** 458
[13] Cordery R, Sarker S and Toboshnik J 1981 *Phys. Rev.* B **24** 5402
[14] da Silva J K L, Moreira A G, Soares M S and Sá Barreto F C 1995 *Phys. Rev.* E **52** 4527
[15] Droz M, da Silva J K L and Malaspinas A 1986 *Phys. Lett.* A **115** 448
[16] Stinchcombe R B, Santos J E and Grynberg M D 1998 *J. Phys. A: Math. Gen.* **31** 541
[17] Pini M G and Rettori A 2007 *Phys. Rev.* B **76** 064407
Pini M G and Rettori A 2007 *Phys. Rev.* B **76** e069903 (erratum)
[18] Ising E 1925 *Z. Phys.* **31** 253
[19] Einax M and Schulz M 2001 *J. Chem. Phys.* **115** 2282
[20] Goodenough J B 1963 *Magnetism and the Chemical Bond* (New York: Interscience)
[21] Goodenough J B 1958 *J. Phys. Chem. Solids* **6** 287
[22] Kanamori J 1959 *J. Phys. Chem. Solids* **10** 87
[23] Siggia E D 1977 *Phys. Rev.* B **16** 2319
[24] Lieb E, Schultz T and Mattis D 1961 *Ann. Phys. NY* **16** 407
[25] Alcaraz F C, Droz M, Henkel M and Rittenberg V 1994 *Ann. Phys.* **230** 250
[26] Mattis D C and Glasser M L 1998 *Rev. Mod. Phys.* **70** 979 and references therein
[27] Lecren L, Wernsdorfer W, Li Y G and Vindigni A 2007 *J. Am. Chem. Soc.* **129** 5045
[28] Vindigni A 2008 *Inorg. Chim. Acta* **361** 3731
[29] Felderhof B U and Suzuki M 1971 *Physica* **56** 43
[30] Kimball J C 1979 *J. Stat. Phys.* **21** 289
[31] Suzuki M and Kubo R 1968 *J. Phys. Soc. Japan* **24** 51
[32] Luscombe J H, Luban M and Reynolds J P 1996 *Phys. Rev.* E **53** 5852
[33] Caneschi A, Gatteschi D, Lalioti N, Sangregorio C, Sessoli R, Venturi G, Vindigni A, Rettori A, Pini M G and Novak M A 2001 *Angew. Chem. Int. Edn* **40** 1760
[34] Caneschi A *et al* 2002 *Europhys. Lett.* **58** 771
Caneschi A, Gatteschi D, Lalioti N, Sangregorio C, Sessoli R, Venturi G, Vindigni A, Rettori A, Pini M G and Novak M A 2002 *Europhys. Lett.* **58** 771
[35] Bernot K, Luzon J, Sessoli R, Vindigni A, Thion J, Richeter S, Leclercq D, Larionova J and van der Lee A 2008 *J. Am. Chem. Soc.* **130** 1619

[36] Bernot K 2007 Lanthanides in molecular magnetism: from mononuclear single molecule magnets to single-chain magnets *PhD Thesis* INSA-Rennes, France
[37] Bernot K, Luzon J, Caneschi A, Gatteschi D, Sessoli R, Bogani L, Vindigni A, Rettori A and Pini M G 2009 *Phys. Rev.* B **79** 134419
[38] Huang K 1987 *Statistical Mechanics* (New York: Wiley)
[39] Brey J J and Prados A 1996 *Phys. Lett.* A **216** 240
[40] Gammaitoni L, Hänggi P, Jung P and Marchesoni F 1998 *Rev. Mod. Phys.* **70** 223
[41] Pandit R and Tannous C 1983 *Phys. Rev.* B **28** 281
[42] Gatteschi D, Caneschi A, Pardi L and Sessoli R 1994 *Science* **265** 1054
[43] Gatteschi D and Sessoli R 2003 *Angew. Chem. Int. Edn* **42** 268 and references therein
[44] Coulon C, Clérac R, Lecren L, Wernsdorfer W and Miyasaka H 2004 *Phys. Rev.* B **69** 132408
[45] Luzon J, Bernot K, Hewitt I J, Anson C E, Powell A K and Sessoli R 2008 *Phys. Rev. Lett.* **100** 247205
[46] Gambardella P, Dallmeyer A, Maiti K, Malagoli M C, Eberhardt W, Kern K and Carbone C 2002 *Nature* **416** 301
[47] Mydosh J A 1993 *Spin Glasses: an Experimental Introduction* (London: Taylor and Francis)
[48] Maignan A, Michel C, Masset A C, Martin C and Raveau B 2000 *Eur. Phys. J.* B **15** 657
[49] Etzkorn S J, Hibbs W, Miller J S and Epstein A J 2004 *Phys. Rev.* B **70** 134419
[50] Bogani L 2005 Magnetic and magneto-optical properties of molecular compounds *PhD Thesis* Università di Firenze, Italy
[51] Girtu M A, Wynn C M, Sugiura K I, Miller J S and Epstein A J 1997 *J. Appl. Phys.* **81** 4410
[52] Cornia A, Fabretti A C, Pacchioni M, Zobbi L, Bonacchi D, Caneschi A, Gatteschi D, Biagi R, Del Pennino U, De Renzi V, Gurevich L and van der Zant H S J 2003 *Angew. Chem. Int. Edn* **42** 1645
[53] Nait Abdi A, Bucher J P, Rabu P, Toulemonde O, Drillon M and Gerbier P 2004 *J. Appl. Phys.* **95** 7345
[54] Mannini M, Pineider F, Sainctavit P, Danieli C, Otero E, Sciancalepore C, Talarico A M, Arrio M-A, Cornia A, Gatteschi D and Sessoli R 2009 *Nature Mater.* **8** 194 and references therein
[55] Piramanayagam S N and Srinivasan K 2009 *J. Magn. Magn. Mater.* **321** 485
[56] Back C H, Allenspach R, Weber W, Parkin S S, Weller D, Garwin E L and Siegmann H C 1999 *Science* **285** 864